# Probability distribution function of tracer differences and the diffusive scale in the stratosphere

Yongyun Hu

Raymond T. Pierrehumbert

Noboru Nakamura

Short title: PDF OF STRATOSPHERIC TRACER DIFFERENCES

**Abstract.** The PDF of $N_2O$ mixing ratio differences over various separation distances is studied using ER-2 airborne data. It is found that the PDF shape ranges from Gaussian, through stretched exponential and exponential, back to Gaussian as the separation distance increases from 200 $m$ to about 200 $km$. With the PDF as a diagnostic tool, we identify the horizontal diffusive scale in the lower stratosphere to be about 2 $km$, and the corresponding vertical diffusivity to be on the order of molecular diffusivity, $1.0 \times 10^{-4}$ $m^2 s^{-1}$. For the typical stretching rate of the stratospheric flow, 0.25 $day^{-1}$, it takes about 25 days to stretch a tracer parcel with initial size of 1000 $km$ into a diffusive-scale filament.

## Introduction

There has been great interest in stratospheric tracer mixing and its effects on ozone chemistry during the last two decades. One of the key problems is the characterization of tracer spatial variability, and specifically, the estimation of the horizontal *diffusive scale*. This is the smallest spatial scale of stratospheric tracers at which molecular diffusion takes place and different chemical species begin to react efficiently [*Juckes and McIntyre,* 1987; *Haynes and Anglade,* 1997]. Recent studies suggested that the horizontal diffusive scale is about 15 $km$ [*Waugh et al.,* 1997; *Balluch and Haynes,* 1997]. However, it has been suggested that this is probably an over-estimate [*Plumb et al.,* 2000].

Power spectra are commonly used to characterize tracer spatial variations. However, a further understanding of tracer mixing requires statistical information beyond power spectra. A more complete characterization of tracer mixing is given by tracer probability distribution functions (PDF's). The recent renaissance of the study of tracer PDF's was stimulated by Rayleigh-Benard convection experiments [*Castaing et al.*, 1989], in which the PDF of temperature fluctuations illustrated a small *Gaussian core* and long *exponential tails*. Theoretical and experimental efforts yielded a fundamental understanding of the way the non-Gaussian tails arise from tracer mixing in turbulent or random flows. In addition to the PDF of tracer itself, there have been studies of the PDF's of tracer gradients and differences over finite separation distances [*Ching,* 1991]. These studies suggested that the PDF of tracer gradients is *stretched exponential*, and

the PDF of tracer differences evolves from stretched exponential to Gaussian when the separation distance increases from dissipation-range to integral-range. The stretched exponential form of the gradient PDF is a result of dissipation, as the undiffused PDF would be lognormal; however, the shape and width of the gradient PDF is insensitive to the magnitude of the diffusion. It is the spatial scale at which the PDF of two-point tracer differences begins to look like the gradient PDF, which provides information about the scales at which dissipation takes place. A survey of key developments in experiments and theories on PDF's can be found in *[Warhaft, 2000]* and [*Majda and Kramer,* 1999; *Pierrehumbert,* 2000], respectively.

The PDF statistics have the potential of being useful in probing the importance of large tracer fluctuations on ozone chemistry. The non-Gaussian tails of tracer PDF's imply that large-amplitude tracer fluctuations have much higher probability than random events governed by Gaussian PDF's and have correspondingly greater impact on chemistry. The PDF's of a passive tracer have been numerically studied using analyzed observational stratospheric winds as driving flows [*Hu and Pierrehumbert, 2001a, 2001b, 2001c*]. The simulation results indeed demonstrated similar non-Gaussian behavior to the above experimental and theoretical results. In the present article we shall study the PDF of nitrous-oxide ($N_2O$) mixing ratio differences using NASA's ER-2 airborne data.

The purpose of this article is twofold. First, we introduce the concept of the PDF of tracer differences and demonstrate why it is more useful than power spectra in characterizing tracer spatial variability. Second, we identify the horizontal diffusive scale and *mixdown time* in the lower stratosphere using the PDF of tracer differences as

a diagnostic tool.

## Theoretical considerations

Tracer advection-diffusion is governed by the equation

$$\frac{\partial \theta}{\partial t} + \mathbf{v} \cdot \bigtriangledown \theta = \kappa \bigtriangledown^2 \theta, \tag{1}$$

where $\theta$ is the mixing ratio of a passive tracer, $\mathbf{v}$ is the velocity of an incompressible flow, and $\kappa$ is diffusivity. For atmospheric applications, we are interested in the large Peclet number limit, $Pe = VL/\kappa \gg 1$, where $V$ and $L$ are the characteristic scales of velocity and the flow eddy-length (integral scale), respectively.

The spatial variation of the tracer can be measured by the difference of tracer concentration over various finite separation scales, $\triangle\theta(r) = \theta(r + r_0) - \theta(r_0)$. Tracer structure functions are defined as

$$S_n(r) = \langle |\triangle\theta(r)|^n \rangle = \langle |\theta(r + r_0) - \theta(r_0)|^n \rangle \,, \tag{2}$$

where the angle bracket $\langle\ \rangle$ denotes ensemble or space averaging, and $n$ is the order of the structure function. The second-order structure function, $S_2(r) = 2\left\{\langle\theta^2\rangle - \langle\theta(r_0)\theta(r + r_0)\rangle\right\}$, provides information equivalent to the tracer power spectrum which is the Fourier transform of the correlation function, $\langle\theta(r_0)\theta(r + r_0)\rangle$. To examine the statistics of anomalously large-amplitude tracer differences, one has to go beyond the second-order structure function or power spectrum and compute higher-order ($n > 2$) structure functions. Structure functions of any order can be

constructed from the PDF of tracer differences, $P(|\triangle\theta|, r)$, that is

$$S_n(r) = \int |\triangle\theta|^n \, P(|\triangle\theta|, r) d(|\triangle\theta|). \tag{3}$$

Therefore, the PDF of tracer differences contains more statistical information than power spectra, and provides a way of characterizing the occurrence of infrequent large-amplitude excursions over various separation scales.

When the separation distance is small, say, close to the diffusive scale, i.e., $r \approx r_d$, diffusion keeps the tracer field smooth, and we have $\triangle\theta \approx \bigtriangledown\theta r_d \propto \bigtriangledown\theta$. Thus, the PDF shape of the tracer differences over $r \approx r_d$ should be similar to that of the tracer gradients, which have *stretched exponential* tails [*Hu and Pierrehumbert,* 2001b]. Over inertial-range distances, i.e., $r_d < r < L$, advection becomes important. In this case, $\langle(\triangle\theta)^2\rangle = 2\left\{\langle\theta^2\rangle - \langle\theta(r_0)\theta(r+r_0)\rangle\right\} \propto Ln\left(\frac{r}{r_d}\right)$, because $\langle\theta(r_0)\theta(r+r_0)\rangle$ is controlled by advection along correlated trajectories extending backwards in time from the two points, i.e., $\langle\theta(r_0)\theta(r+r_0)\rangle \propto Ln\left(\frac{L}{r}\right)$, and $\langle\theta^2\rangle \propto Ln\left(\frac{L}{r_d}\right)$. Therefore, $P(\triangle\theta, r)$ should be similar to the one-point tracer PDF, $P(\theta)$, except for replacing $Ln\left(\frac{L}{r_d}\right)$ with $Ln\left(\frac{r}{r_d}\right)$ in *Chertkov et al.*'s [1995] analysis, that is, $P(\triangle\theta, r)$ has a Gaussian core and exponential tails. Over integral-range distances (e.g. eddy-length or $r \approx L$), tracer concentrations at the two points are nearly uncorrelated, i.e., $\langle\theta(r_0)\theta(r+r_0)\rangle \approx 0$, so that $P(\triangle\theta, r)$ is the convolution of the one-point tracer PDF with itself. But in this case, the convolution emphasizes the Gaussian core of the one-point PDF, pushing the transition to exponential tails out to very extreme values; in consequence the difference PDF looks quite Gaussian. For $r \ll r_d$ (sub-dissipation-range), the difference PDF for a

smooth tracer field should in principle also look like the gradient PDF for $r \approx r_d$. But we shall see that there is evidence that the observed $N_2O$ differences at this scale are governed by distinct physics, and again become Gaussian.

The PDF's in all ranges are members of the stretched-exponential family

$$P(\triangle\theta, r) \propto \exp(-\beta\,|\triangle\theta|^{\gamma}), \tag{4}$$

where $\gamma$ is called the *stretching parameter*, and $\beta$ is a dimensionless coefficient related to the ratio of the mean value and standard deviation of Lyapunov exponents [*Hu and Pierrehumbert,* 2001b]. The stretching parameter is a function of $r$ and ranges within $0 \leq \gamma \leq 2$. The smaller $\gamma$ is, the more wildly fluctuating the tracer difference field becomes. When $\gamma < 1$, $P(\triangle\theta, r)$ is stretched exponential. $\gamma = 1,\ 2,\ 0$ corresponds to exponential, Gaussian, and algebraic tails (for a decaying passive tracer), respectively.

## PDF's of $N_2O$ differences

The $N_2O$ mixing ratio data used for this study are from two ER-2 flight missions in NASA's Stratospheric Tracers of Atmospheric Transport (STRAT) project. The accuracy of $N_2O$ mixing ratio is approximately $\pm 2\%$ ($\pm 3$ *ppbv*) for 1 Hz measurements recorded by the airborne tunable laser absorption spectrometer (ATLAS) [*Podolske and Loewenstein,* 1993]. The normal cruise speed of the ER-2 aircraft is about 200 $ms^{-1}$, so that 1 Hz corresponds to a spatial resolution of about 200 $m$. The cruise altitude for the two missions is about 20$km$. The first mission was from Ames toward north to 60°N and back to Ames, California (hereafter, mission 950508), and the second one was

a transit flight from Hawaii to Ames (hereafter, 961213).

Fig. 1 shows the PDF's of $N_2O$ differences calculated from the mission 950508. At $r \approx 200\ m$ (Fig. 1**A**), the PDF is stretched exponential; the tails can be fit by a stretched exponential curve, with the stretching parameter $\gamma \approx 0.56$. At $r \approx 2\ km$ (Fig. 1 **B**), the stretched exponential tails become flatter, with $\gamma = 0.45$. At $r \approx 90\ km$ (Fig. 1 **C**), the PDF shows exponential tails ($\gamma = 1.0$). For a much larger distance, say, $r \approx 160\ km$ (Fig. 1**D**), the PDF becomes Gaussian ($\gamma = 2$). The variation of the stretching parameter $\gamma$ as a function of $r$ is illustrated in Fig. 2. There is a turning point where $\gamma$ reaches a minimum. For $r < 2$ km, $\gamma$ rapidly drops from 0.56 to 0.4, then quickly increases up to 1.0 at $r \approx 90\ km$. Beyond that, $\gamma$ slowly increases and eventually reaches 2 at $r \approx 160\ km$. The behavior of $\gamma$ near the turning point is enlarged in the inset, with a minimum $\gamma \approx 0.4$ at $r \approx 1.6\ km$.

As $r > 2\ km$, the evolution of the stretching parameter is similar to the observations in turbulence experiments [*Ching,* 1991; *Warhaft,* 2000]. However, our result for $r < 2\ km$ is different from that in Rayleigh-Benard convection experiments in which the stretching parameter reaches a saturation value of about 0.5 at small scales [*Ching,* 1991]. For our case, the increase of the stretching parameter means that $N_2O$ mixing ratio field again becomes non-smooth at small scales, perhaps as a result of gravity wave breaking or fully 3-dimensional turbulence. This is consistent with the roughly $k^{-2}$ power spectrum [*Shepherd,* 1997].

The PDF's of $N_2O$ differences from the second mission (hereafter mission 961213) have similar shapes to the above over the same separation distances (not shown). The

variation of the stretching parameter $\gamma$ as a function of $r$ is shown in Figure 3. At $r \approx 200\ m$, $\gamma \approx 2$. The turning point is located at $r \approx 2\ km$, with a minimum value $\gamma \approx 0.5$.

In both missions, the common significance is that the stretching parameter $\gamma$ experiences a minimum at a comparable separation scale, $r \approx 2\ km$, at which the $N_2O$ difference field has the highest relative probability of extreme excursions. Below this scale, the difference field becomes less wildly fluctuating, and the PDF tends towards Gaussian. This implies that at $r \approx 2\ km$ the horizontal stretching of $N_2O$ filaments is checked by strong small scall dissipation. Therefore, the turning point is indicative of the horizontal diffusive scale for passive stratospheric tracers. Another common feature is the "knee" at $r \approx 20\ km$ ($r/r_0 = 100$). This is an indicative of the transition from the dissipation to inertial-range.

The differences between the two missions are: the minimum value of $\gamma$ in mission 950508 ($\gamma = 0.4$) is smaller than that in mission 961213 ($\gamma = 0.5$), and the corresponding separation distance is also smaller. In addition, the PDF of $N_2O$ differences at $r \approx 200\ m$ is close to Gaussian. This suggests that the $N_2O$ differences at the diffusive scale in mission 950508 (along the meridional direction) are more wildly fluctuating than that in mission 961213 (approximately along the zonal direction). This may be because the zonal-wind shear ($\frac{\partial \bar{u}}{\partial y}$) of stratospheric flow tends to homogenize zonal tracer variations rapidly.

Note that the PDF's of $N_2O$ differences from the ER-2 airborne data only reflects the situations of the stratosphere within a limited distance-range, i.e., from

sub-dissipation-, through dissipation-, to the lower part of inertial-ranges of separation distances. Our simulations gave a global view of the tracer difference PDF's [*Hu and Pierrehumbert,* 2001c].

## The diffusive scale and mixdown time

The diffusive scale of a passive tracer is determined by the balance between outward diffusion and stretching. As a result,

$$r_d = \sqrt{\frac{\kappa}{\lambda}}, \tag{5}$$

where $\lambda$ is the stretching rate or Lyapunov exponent. For the lower stratospheric flow, the typical value of horizontal stretching rate (e.g. the mean Lyapunov exponent) is about $\bar{\lambda} = 0.25\ day^{-1}$ [*Hu and Pierrehumbert,* 2001a]. Substitution of this value and $r = 2\ km$ into (5) yields a diffusivity $\kappa \approx 10\ m^2 s^{-1}$, which is surely orders of magnitude greater than molecular diffusivity. This suggests that such a horizontal scale is not a result of direct action molecular diffusivity.

This discrepancy has been noted in [*Juckes and McIntyre,* 1987] and later quantitatively studied in [*Haynes and Anglade,* 1997]. The latter suggested that while a stratospheric tracer is exponentially stretched into small scales on quasi-horizontal isentropic surfaces at the rate of $\bar{\lambda}$, the vertical scales is tilted by vertical wind shear $\Gamma = \partial\bar{u}/\partial z$, and that the characteristic aspect ratio between horizontal and vertical tracer scales is $\alpha = r/h = \Gamma/\bar{\lambda}$. Their scaling analysis and estimation using observed stratospheric winds gave $\alpha \approx 250$ [*Haynes and Anglade,* 1997]. Thus, the vertical

scale of the tracer is always much smaller than the horizontal scale and is first checked by molecular diffusion. While diffusion takes place on the vertical diffusive scale, $h_d$, the corresponding horizontal diffusive scale is $r_d = \alpha h_d$. It is as if there were a "horizontal diffusivity" $\kappa_H$ acting on $r_d$. There is the relation $\kappa_H = \alpha^2 \kappa_V$, where $\kappa_V$ indicates molecular diffusivity in the vertical direction. Substitution of $r_d \approx 2\ km$, $\kappa_H = 10\ m^2 s^{-1}$, and $\alpha = 250$ into (5) yields $h_d \approx 8\ m$ and $\kappa_V \approx 1.0^{-4}\ m^2 s^{-1}$ which is approximately on the order of molecular diffusivity (for air molecules in the stratosphere [*Haynes and Anglade,* 1997]). Therefore, $r_d \approx 2\ km$ is indeed the horizontal diffusive scale which is determined by molecular diffusivity acting on the vertical structures that have been tilted by the vertical wind shear, but not by molecular diffusivity acting in the horizontal direction. This diffusive scale suggests that the mixdown time for a stratospheric tracer parcel from an initial horizontal scale of $L = 1000\ km$ to $r_d \approx 2\ km$ is $t^* = \frac{1}{\lambda} \log\left(\frac{L}{r_d}\right) \approx 25$ days.

One might expect to determine the diffusive scale by finding a diffusive cut-off from tracer power spectra. However, the $N_2O$ power spectra in [*Strahan and Mahlman,* 1994; *Bacmeister et al.,* 1996] do not show a clear diffusive cut-off. This is probably because the ensemble average, $\langle \theta(r_0)\theta(r + r_0)\rangle$, for computing power spectra smoothes out large-amplitude tracer differences between low and high strains. In contrast, the PDF is able to focus on the large-amplitude tracer differences at various separation distances; in particular, the variation of the PDF shape (e.g. the stretching parameter $\gamma$) with separation distances displays a clear indication of the diffusive scale. The PDF analysis in essence diagnoses the diffusive scale by using the anomalous events

constituting the tails of the PDF as a prove for the effect of diffusion.

## Conclusion

We have studied the PDF of $N_2O$ differences measured by the NASA ER-2 aircraft. It is found that the results are generally in agreement with the theoretical predictions. The PDF shape evolves from Gaussian through stretched exponential, exponential, back to Gaussian as the separation distance increases from 200 $m$ to about 200 $km$. Using the PDF as a diagnostic tool, we have identified the horizontal diffusive scale in the lower stratosphere to be about 2 $km$, which is attributed to vertical diffusion, with magnitude on the order of molecular diffusivity, $10^{-4}$ $m^2s^{-1}$. The mixdown time for a tracer parcel, with initial size of 1000 $km$, to be stretched to the diffusive scale is about 25 days.

**Acknowledgments.** We are grateful to Peter Haynes and Alan Plumb for their reading the draft and helpful comments. We also thank Jun Ma and Doug Allen who provided us with the ER-2 data. Y.H. and R.T.P. are supported by the ASCI Flash Center at the University of Chicago under DOE contract B341495, and by the National Science Foundation under grant ATM9505190. N.N. is supported by the NASA grant NAGS-6693.

## References

Bacmeister, J. T., and Co-authors, Stratospheric horizontal wavenumber spectra of winds, potential temperature, and atmospheric tracers observed by high-altitude aircraft, *J. Geophys. Res., 101,* 9441-9470, 1996.

Balluch, M. G., and P. H. Haynes, Quantification of lower stratospheric mixing processes using aircraft data, *J. Geophy. Res., 102*, 23487-23504, 1997.

Castaing, B., and Co-authors, Scaling of hard thermal turbulence in Rayleigh-Benard convection, *J. Fluid Mech., 204,* 1-30, 1989.

Chertkov, M., G. Falkovich, I. Kolokolov, and I. Lebedev, Statistics of a passive scalar advected by a large-scale two-dimensional velocity field: analytic solution, *Phys. Rev. E, 51,* 5609-5627, 1995.

Ching, E. S. C., Probabilities for temperature differences in Rayleigh-Benard convection, *Phys. Rev. A, 44*, 3622-3629, 1991.

Haynes, P. H., and J. Anglade, The vertical-scale cascade in atmospheric tracers due to large-scale differential advection, *J. Atmos. Sci., 54,* 1121-1136, 1997.

Hu, Y., and R. T. Pierrehumbert, The advection-diffusion problem for stratospheric flow, Part I: Concentration probability distribution function, *J. Atmos. Sci,* in press, 2001a.

Hu, Y., and R. T. Pierrehumbert, The advection-diffusion problem for stratospheric flow, Part II: Probability distribution function of tracer gradients, to be submitted to *J. Atmos. Sci.,* 2000b.

Hu, Y., and R. T. Pierrehumbert, The advection-diffusion problem for stratospheric flow, Part

III: Probability distribution function of tracer differences, to be submitted to *J. Atmos. Sci.,* 2000c.

Juckes M. N., and M. E. McIntyre, A high-resolution one-layer model of breaking planetary waves in the stratosphere, *Nature, 328,* 590-596, 1987.

Majda, A. J., and P. R. Kramer, Simplified models for turbulent diffusion: Theory, numerical modeling, and physical phenomena, *Phys. Rep., 314,* 237-574, 1999.

Pierrehumbert, R. T., Lattice models of advection-diffusion, *Chaos, 10,* 61-74, 2000.

Plumb, R. A., D. W. Waugh, and M. P. Chipperfield, The effects of mixing on tracer relationships in the polar vortices, *J. Geophys. Res., 105,* 10047-10062, 2000.

Podolske, J. R., and M. Loewenstein, Airborne tunable diode laser spectrometer for trace gas measurements in the lower stratosphere, *Appl. Opt., 32,* 5324-5333, 1993.

Shepherd, T. G., Transport and mixing in the lower stratosphere: a review of recent developments, *SPARC Newsletter, 9,* 1997.

Strahan, S. E., and J. D. Mahlman, Evalution of the SKYHI general circulation model using aircraft $N_2O$ measurements, Part II: Tracer variability and diabatic meridional circulation, *J. Geophys. Res., 99,* 10319-10332, 1994.

Warhaft, Z., Passive scalars in turbulent flows, *Annu. Rev. Fluid Mech., 32*, 203-240, 2000.

Waugh, D. W., and Co-authors, Mixing of polar vortex air into middle latitudes as revealed by tracer-tracer scatter plots, *J. Geophys. Res., 102,* 13119-13134, 1997.

---

Y. Hu, R. T. Pierrehumbert, and N. Nakamura, Department of the

Geophysical Sciences, University of Chicago, Chicago, IL 60637. (e-mail: yongyun@amath.washington.edu; rtp1@geosci.uchicago.edu; nnn@bethel.uchicago.edu)

Received _____

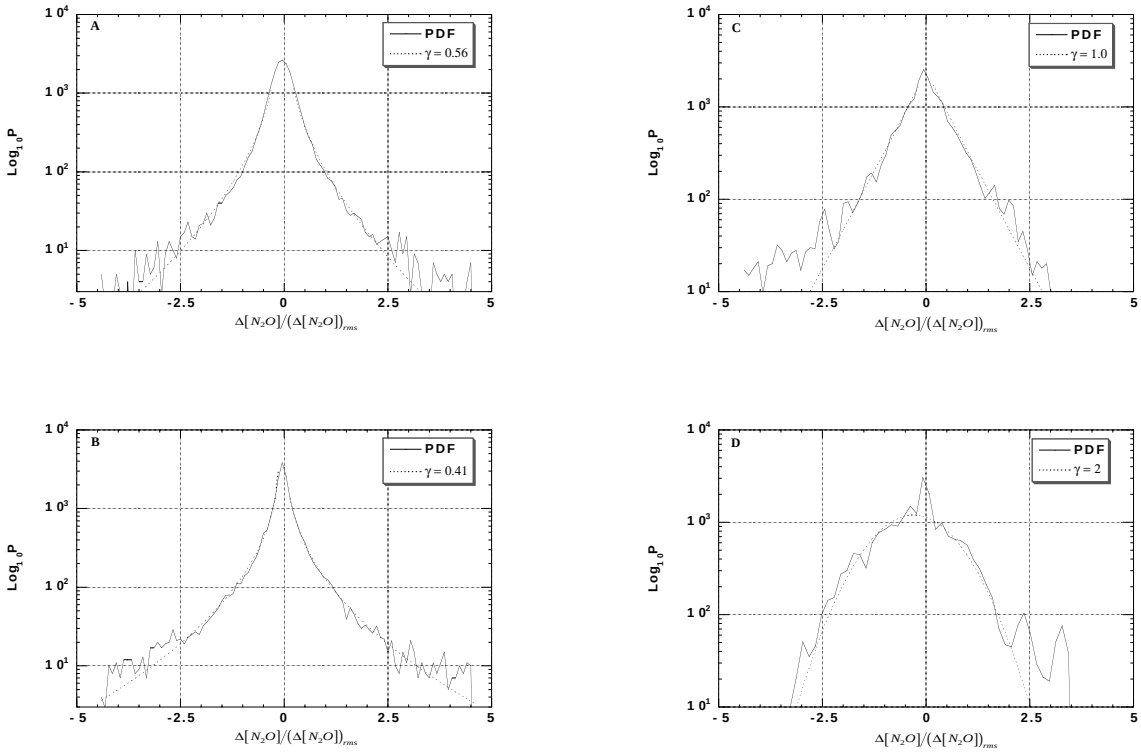


**Figure 1.** PDF's of $N_2O$ mixing ratio differences calculated from mission 950508. The vertical axis is in logarithm, and the horizontal axis is normalized by the root-mean-square (rms) of $N_2O$ differences. The solid-lines are the PDF curves, and the dotted-lines are fitting curves. $\gamma$ is the stretching parameter for fitting the PDF curves. (**A**) $r \approx 0.2$ km, (**B**) $r \approx 2$ km, (**C**) $r \approx 90$ km, (**D**) $r \approx 160$ km.

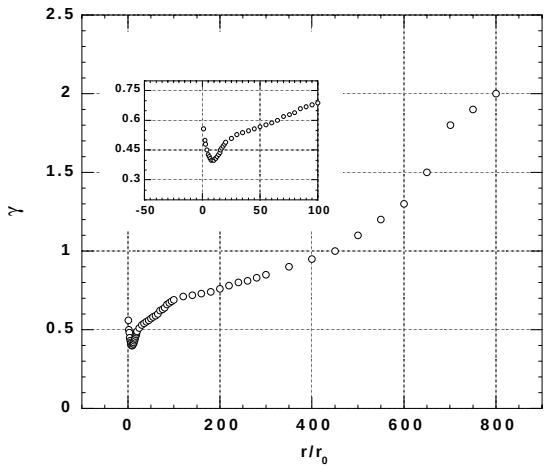


**Figure 2.** Variation of stretching parameter $\gamma$ for mission 950508, as a function of separation distance $r/r_0$, where $r_0 \approx 200$ m. The inset is an enlarged plot to illustrate the variation near the turning point.

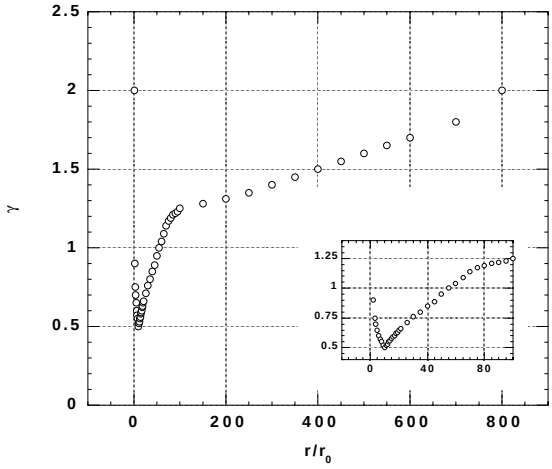


**Figure 3.** Same as Fig. 2, except for mission 961213.